CrossMark

RESEARCH ARTICLE

# Increased hepatic fatty acid polyunsaturation precedes ectopic lipid deposition in the liver in adaptation to high-fat diets in mice

Ana Francisca Soares[1] · João M. N. Duarte[1] · Rolf Gruetter[1,2,3]

## Abstract

*Objective* We monitored hepatic lipid content (HLC) and fatty acid (FA) composition in the context of enhanced lipid handling induced by a metabolic high-fat diet (HFD) challenge and fasting.

*Materials and methods* Mice received a control diet (10% of kilocalories from fat, $N = 14$) or an HFD (45% or 60% of kilocalories from fat, $N = 10$ and $N = 16$, respectively) for 26 weeks. A subset of five mice receiving an HFD (60% of kilocalories from fat) were switched to the control diet for the final 7 weeks. At nine time points, magnetic resonance spectroscopy was performed in vivo at 14.1 T, interleaved with glucose tolerance tests.

*Results* Glucose intolerance promptly developed with the HFD, followed by a progressive increase of fasting insulin level, simultaneously with that of HLC. These metabolic defects were normalized by dietary reversal. HFD feeding immediately increased polyunsaturation of hepatic FA, before lipid accumulation. Fasting-induced changes in hepatic lipids (increased HLC and FA polyunsaturation, decreased FA monounsaturation) in control-diet-fed mice were not completely reproduced in HFD-fed mice, not even after dietary reversal.

*Conclusion* A similar adaptation of hepatic lipids to both fasting and an HFD suggests common mechanisms of lipid trafficking from adipose tissue to the liver. Altered hepatic lipid handling with fasting indicates imperfect metabolic recovery from HFD exposure.

**Keywords** Insulin resistance · Liver · Nuclear Magnetic Resonance · Nutrition · Obesity · Polyunsaturated fat

## Introduction

The sedentary lifestyle and unrestricted intake of high-caloric food products experienced currently in Western societies has caused obesity to reach pandemic proportions [1]. The economic, social, and health burdens of this phenomenon are further aggravated by associated metabolic diseases, notably type 2 diabetes [2]. High-fat diet (HFD) feeding is a widely used experimental model to study obesity and its associated metabolic complications. It has been established that prolonged exposure to an HFD not only causes obesity but also compromises liver and adipose tissue physiology, and perturbs beta-cell function [3–6].

Obesity represents a situation of positive whole-body energy balance that favors energy storage and ultimately ectopic deposition in the liver. The liver is a major participant in whole-body metabolism, and the progression of metabolic disease is largely determined by hepatic lipid handling. In the liver, lipid intermediates are involved in molecular mechanisms that lead to hepatic insulin resistance and hyperglycemia [7]. On the other hand, hepatic lipid accumulation without obesity has also been reported on short-term exposure to an HFD in both rodents [8, 9] and healthy humans [10, 11].

✉ Ana Francisca Soares
  francisca.soares@epfl.ch

1   Laboratory for Functional and Metabolic Imaging, Swiss Federal Institute of Technology, Bâtiment CH, Station 6, 1015 Lausanne, Switzerland

2   Department of Radiology, University of Geneva, Geneva, Switzerland

3   Department of Radiology, Faculty of Biology and Medicine, University of Lausanne, Lausanne, Switzerland

Studies with genetically modified mice report that increased storage of triglycerides per se does not have a deleterious effect on insulin sensitivity [12, 13]. However, and in contrast to these models, hepatic lipid accumulation on HFD feeding is not an essential hepatic defect but rather a result of increased fatty acid (FA) uptake [14, 15]. In addition, an early association between HFD feeding and hepatic insulin resistance has been reported [8, 9, 16]. Increased hepatic FA influx leading to lipid accumulation is also observed with prolonged fasting, on mobilization of adipose stores [17–19], but in this case hepatic insulin resistance is not present [18]. Thus, alterations in the hepatic lipid pool are a physiological response to increased circulating FA levels, and are not necessarily associated with changes in insulin sensitivity.

Not only the amount of fat in the diet but also its qualitative FA composition influences the extent of hepatic FA uptake, hepatic FA accumulation, and ensuing metabolic defects. It has been shown that diets rich in saturated FA (SFA) cause greater metabolic damage than those rich in monounsaturated FA (MUFA) or polyunsaturated FA (PUFA) [6, 20, 21]. Although the unsaturation features of FA in hepatic triglycerides were shown to mirror those of the diet after long-term exposure in rats [21], tracer methods found that dietary fat is not the major source of hepatic lipids during exogenous lipid delivery [22–24]. Hence, it remains to be fully elucidated how the composition of the hepatic FA pool progressively adapts to changes in dietary fat, and whether there is a relation with metabolic variables during this adaptation.

In the present study we aimed at elucidating the evolution of the hepatic lipid signature in the context of HFD-induced metabolic damage, noninvasively, by proton magnetic resonance spectroscopy ($^1$H-MRS) in vivo over a period of 26 weeks in mice. In anticipation of an effect of dietary fat load on the phenotype, mice were exposed to diets whose composition differed in the amount of lard-derived fat component (rich in SFA). We further evaluated the reversibility of the HFD-induced phenotype by performing a dietary switch from an HFD to the control diet for the final 7 weeks of the study in a subset of mice. In addition, we also investigated the adaptation of hepatic lipids to fasting, when endogenous lipid trafficking is physiologically enhanced, and whether this adaptation would be sensitive to the dietary interventions.

## Materials and methods

### Animal protocol

Animal experiments were performed with the approval by the local ethics committee (Service de la Consommation et des Affaires Vétérinaires, Epalinges, Switzerland). Eleven-week-old male C57BL/6J mice (Charles River Laboratories,

L'Arbresle, France) were housed with a 12-h light, 12-h dark cycle (lights on from 7 a.m.) and allowed 1 week of acclimatization before experiments. The experimental design is depicted in Fig. 1. Mice were allowed free access to water and diets with variable fat content: CD, $N = 14$, control diet with 10% of kilocalories from fat (D12450B, Research Diets, New Brunswick, NJ, USA); HFD45, $N = 10$, an HFD with 45% of kilocalories from fat (D12451, Research Diets, New Brunswick, NJ, USA); HFD60, $N = 16$, an HFD with 60% of kilocalories from fat (D12492, Research Diets, New Brunswick, NJ, USA). The full composition and FA profile of the diets is available at http://www.researchdiets.com/opensource-diets/stock-diets/dio-series-diets. Briefly, the SFA/MUFA/PUFA percent composition was 22.7:29.9:47.4 in CD, 31.4:35.5:33.1 in HFD45, and 32.0:35.9:32.0 in HFD60. All mice received the control diet during acclimatization and received the experimental diets for at least 26 weeks. A diet-induced metabolic phenotype was clearly installed at week 18, and we investigated its reversibility in a subset of mice in the HFD60 group (the group with the severest phenotype) by subjecting them to a dietary reversal to CD for the last 7 weeks (HFD60→CD, $N = 5$). Noninvasive $^1$H-MRS of the liver (see later) and oral glucose tolerance tests (OGTTs; 1.5 g/kg after a 6-h fast) were performed before exposure to the experimental diets (baseline) and after 1, 4, 9, 18, and 26 weeks (Fig. 1). Additional measurements
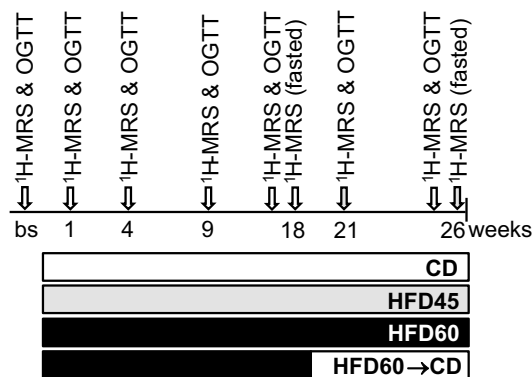


**Fig. 1** Experimental design. Mice were randomly assigned to four dietary regimens: CD (10% of kilocalories from fat, $N = 15$), HFD45 (45% of kilocalories from fat, $N = 10$), HFD60 (60% of kilocalories from fat, $N = 16$ until week 19 and $N = 11$ thereafter), and HFD60→CD (19 weeks of HFD60 followed by 7 weeks of CD, $N = 5$). At the baseline (bs) all groups had access to the control diet (CD). White arrows indicate the time points for experimental assessments in all groups, and gray arrows indicate time points for experimental assessments in the HFD60→CD group exclusively. Proton magnetic resonance spectroscopy ($^1$H-MRS) was performed in vivo, longitudinally, for hepatic lipid characterization; and oral glucose tolerance tests (OGTTs) were done after a minimum 3-day resting period subsequent to the magnetic resonance session. If not otherwise stated, $^1$H-MRS measurements were performed with the mice in the fed state

were performed at week 21 in the HFD60→CD group. Mice were allowed at least 3 days of rest between manipulations, and the time points in Fig. 1 represent the average testing times. Longitudinal $^1$H-MRS was performed in mice fed ad libitum, and an additional measurement was performed after an overnight fast at around week 18 in CD, HFD45, and HFD60 mice, and after dietary reversal, at around week 26, in the HFD60→CD group. At the end of the study, mice anesthetized with isoflurane were killed by cervical dislocation, blood was collected from the descending aorta for biochemical measurements, the livers were removed and immediately freeze-clamped in liquid-nitrogen-cooled metal thongs, and epididymal white adipose tissue (EWAT) was collected and weighed. Livers and plasma were stored at − 80 °C until further processing.

## Hepatic lipid content and FA composition by $^1$H-MRS in vivo

Mice were anesthetized with isoflurane (4% for induction and 1–2% thereafter, in 70:30 air/oxygen), and placed in an in-house-built holder. Body temperature was continuously assessed by a rectal probe and maintained at 36–37 °C by a circulating warm water system. Respiratory rate was kept at 60–90 bpm by regulation of isoflurane delivery, and was continuously monitored with a magnetic resonance (MR)-compatible system (SA Instruments, Stony Brook, NY, USA), which also delivered the necessary triggering signals for respiratory gating during the MR acquisitions. Mice were scanned in the supine position in a 26-cm horizontal bore 14.1-T magnet interfaced with a VNMRS DirectDrive console (Varian, Palo Alto, CA, USA). A $^1$H quadrature surface coil (two 13-mm-inner-diameter physically decoupled loops) placed over the abdomen was used as the transreceiver. Automatic shimming to reduce magnetic field inhomogeneities was performed with FAST(EST)MAP [25]. Multislice gradient echo images were acquired in the sagittal, axial, and coronal orientations (85° flip angle, 25 mm × 25 mm field of view, 128 × 128 data matrix, and minimum repetition and echo times) for identification of the liver and definition of a $(2 \times 2 \times 2)$ mm$^3$ volume of interest for $^1$H-MRS. For consistency, this volume was selected from the right medial lobe, which was identified visually by the experienced observer. Hepatic lipid content (HLC) was determined from localized $^1$H-MR spectra acquired with the stimulated echo acquisition mode (STEAM) technique (8-ms echo time, 20-ms mixing time, 6.5-s repetition time, 4096 complex points, 32 scans) as the peak area of methylene protons at 1.3 ppm (Lip 1.3) relative to that of water plus Lip 1.3, with corrections for differences in spin–spin relaxation times as previously described [26]. The FA composition of intrahepatic lipids was characterized as previously described [26] with use of indices for saturation, number of double bonds, unsaturated

**Table 1** Fatty acid composition indices derived from proton magnetic resonance spectra of hepatic lipids

| Fatty acid composition index | Expression |
| --- | --- |
| Saturation index | $\frac{\text{Lip } 1.3 \times 3}{\text{Lip } 0.9 \times 2}$ |
| Number of double bonds[a] | $\frac{\text{Lip } 5.3 \times 3}{\text{Lip } 0.9 \times 2} \times 1.15$ |
| UFA | $\frac{\text{Lip } 2.1 \times 3}{\text{Lip } 0.9 \times 4}$ |
| SFA | $1 - \text{UFA}$ |
| PUFA or polyunsaturated bonds per fatty acid | $\frac{\text{Lip } 2.8 \times 3}{\text{Lip } 0.9 \times 2}$ |
| MUFA | $\text{UFA} - \text{PUFA}$ |
| Mean chain length | $\frac{1/2(\text{Lip } 1.3 + \text{Lip } 2.1 + \text{Lip } 2.8) + \text{Lip } 5.3}{1/3 \times \text{Lip } 0.9} + 4$ |

Chemically distinct fatty acyl protons are identified by their chemical shift in the proton magnetic resonance spectrum (see also Fig. 5a). For example, Lip 1.3 refers to the methylene protons at 1.3 ppm.

*MUFA* monounsaturated fatty acids, *PUFA* polyunsaturated fatty acids, *SFA* saturated fatty acids, *UFA* unsaturated fatty acids

[a] A correction factor of 1.15 [1/(1 − 0.13)] was used to account for an approximately 13% underestimation of the number of double bonds with our acquisition parameters [1].

FA, SFA, PUFA, MUFA, and mean chain length (Table 1). These indices were obtained from different lipid resonances in spectra acquired with STEAM (2.8-ms echo time, 20-ms mixing time, 5-s repetition time, 2048 complex points, and 86–128 scans) in combination with water suppression and outer volume saturation [27]. Individual spectra were corrected for $B_0$ drift and phase, summed, and analyzed with LCModel version 6.3-1E (LCMODEL) with use of SPTYPE liver-11 with automatic metabolite simulation.

## Biochemical measurements

Blood glucose during the OGTT was measured from the tail tip with a glucometer (Breeze, Bayer, Zurich, Switzerland). Plasma hormones and metabolites were quantified with commercially available kits for insulin ELISA (Mercodia, Uppsala, Sweden), nonesterified FA (NEFA; Wako Chemical, Neuss, Germany), triglycerides (Analox, Stokesley, UK), leptin ELISA (Abcam, Cambridge, UK), adiponectin ELISA (Adipogen, Epalinges, Switzerland), and C-peptide ELISA (Crystal Chem, Downers Grove, USA). Blood alanine transaminase (ALT) and aspartate transaminase (AST) levels were determined with a Reflotron blood analyzer (Roche Diagnostics, Rotkreuz, Switzerland).

## Statistics

Numeric data are the mean ± standard error of the mean. For a given variable, differences between groups were assessed with a one-way ANOVA followed by Newman–Keuls

multiple comparison post hoc tests. A two-way ANOVA (with repeated measures) followed by Student's $t$ test corrected for multiple comparisons was used to assess differences when variables were measured over time. For comparisons of hepatic lipid parameters between the fasted and fed states, for each group a Student $t$ test was performed with corrections for multiple comparisons. Statistical significance was indicated by $P < 0.05$. Correlations were assessed with the Pearson $r$ coefficient.

## Results

A phenotype of obesity, associated with perturbed metabolic variables, was clearly observed in mice fed HFD formulas. Body weight was significantly higher in mice exposed to an HFD than in those exposed to CD, without differences in the average caloric intake per mouse during the 26-week experimental period (Fig. 2). On the other hand, within 1 week of the reversal from HFD60 to CD (HFD60→CD group), caloric intake decreased to $3.8 \pm 0.2$ kcal/day ($P < 0.001$, Fig. 2), along with a significant reduction of body weight from $48.5 \pm 1.0$ g to $43.5 \pm 2.3$ g ($P < 0.05$, Fig. 2). Afterwards, caloric intake in the HFD60→CD group
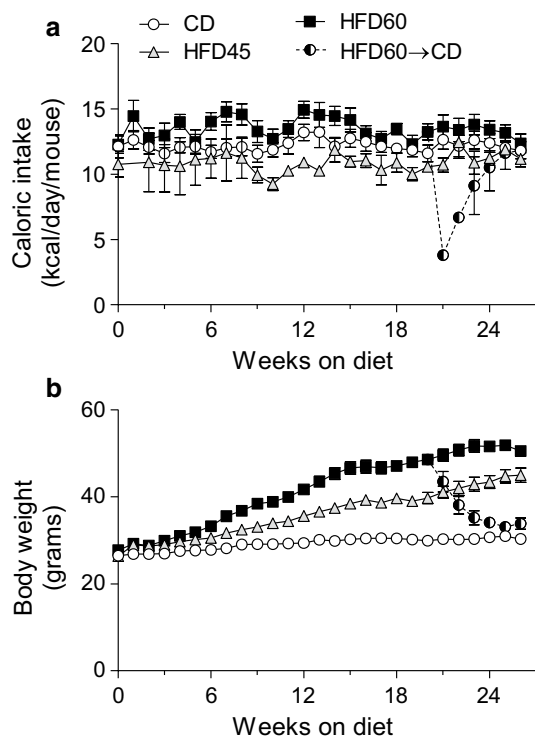


**Fig. 2** Caloric intake (**a**) and body weight (**b**) during 26 weeks of exposure to experimental diets. CD control diet with 10% of kilocalories from fat, HFD45 high-fat diet with 45% of kilocalories from fat, HFD60 high-fat diet with 60% of kilocalories from fat, HFD60→CD HFD60 for 19 weeks followed by CD for 7 weeks

progressively increased to levels similar to those observed in the other dietary groups, while body weight continued to decrease and reached values similar to those in the CD group at the end of the study (Fig. 2). Glucose tolerance was also significantly perturbed by HFD feeding (Fig. 3a). Blood glucose level 2 h after the OGTT was higher in the HFD60 group than in the CD group by week 1 ($P < 0.05$) and remained well above the CD group values until the end of the study (Fig. 3b.). In parallel, the area under the curve for the entire period of the OGTT was also systematically higher in the HFD60 group than in the CD group (Fig. 3c). In the HFD45 group, blood glucose level 2 h after the OGTT was increased relative to that in the CD group at week 4 ($P < 0.01$), week 9 ($P < 0.01$), and week 26 ($P < 0.01$) but not significantly at week 18 ($P = 0.1$ after correction for multiple comparisons, Fig. 3b). Increases in the area under the curve reached statistical significance only by week 26 in the HFD45 group when compared with the CD group (Fig. 3c). After a 6-h fast, blood glucose levels in the HFD60 group were higher than those in the CD group from week 9 ($P < 0.01$) onward, while in the HFD45 group the levels were higher than in the CD group at weeks 18 and 26 ($P < 0.01$, Fig. 3d). Comparatively, fasting plasma insulin level progressively increased relative to that in the CD group in the HFD45 and HFD60 groups from week 4 (Fig. 3e). Taken together, these data show that perturbations of glucose homeostasis, indicated by glucose intolerance and/or altered fasting blood glucose and plasma insulin levels, were detected within a few weeks of HFD feeding and were sustained thereafter. In addition, derangements in the HFD60 group had an earlier onset than those in the HFD45 group, and with time developed to be more pronounced. Similar to our observations for body weight, dietary reversal resulted in the recovery of glucose homeostasis. Fasting blood glucose levels were normalized within 2 weeks ($P < 0.0001$ vs HFD60 group at week 18, Fig. 3d), while the recovery of fasting plasma insulin levels occurred gradually ($P < 0.05$, HFD60→CD group at week 21 vs HFD60 group at week 18; and $P < 0.01$, HFD60→CD group at week 26 vs HFD60 group at week 18; Fig. 3e). Fasting plasma insulin level in the HFD60→CD group was similar to that in the CD group by week 26 (Fig. 3e). Performance during the OGTT was completely normalized by the end of the study in the HFD60→CD group (Fig. 3a–c).

At the end of the study, additional metabolic data were collected from postmortem measurements. Mice in the HFD45 and HFD60 groups displayed higher amounts of EWAT than mice in the CD group, and accordingly higher levels of circulating leptin but no differences in the levels of adiponectin (Table 2). The levels of NEFA in the plasma were also increased in the HFD45 and HFD60 groups relative to the CD group (Table 2), indicating inappropriate control of adipose tissue lipolysis. On the other hand, plasma
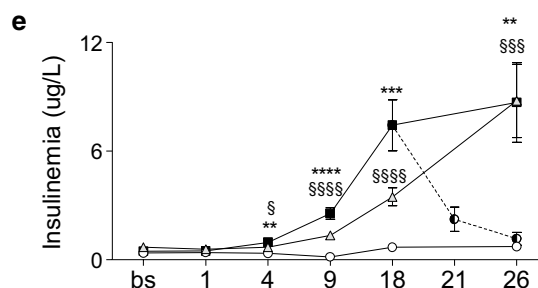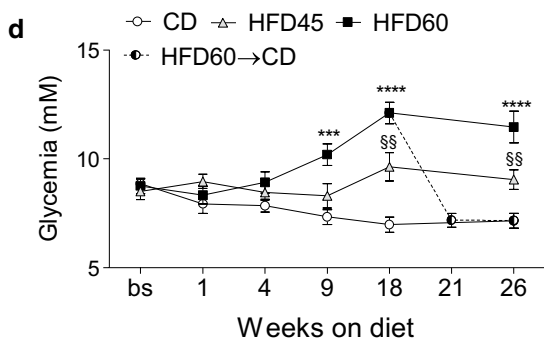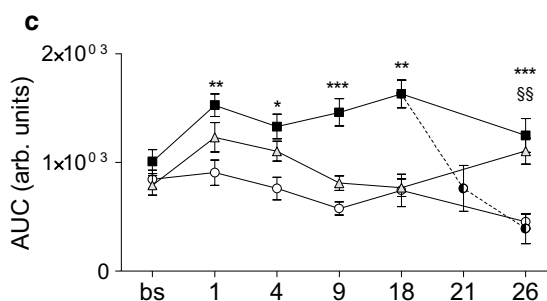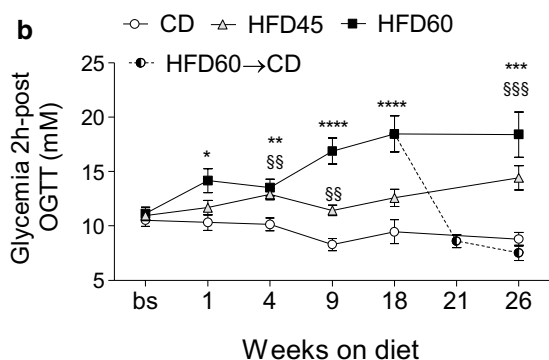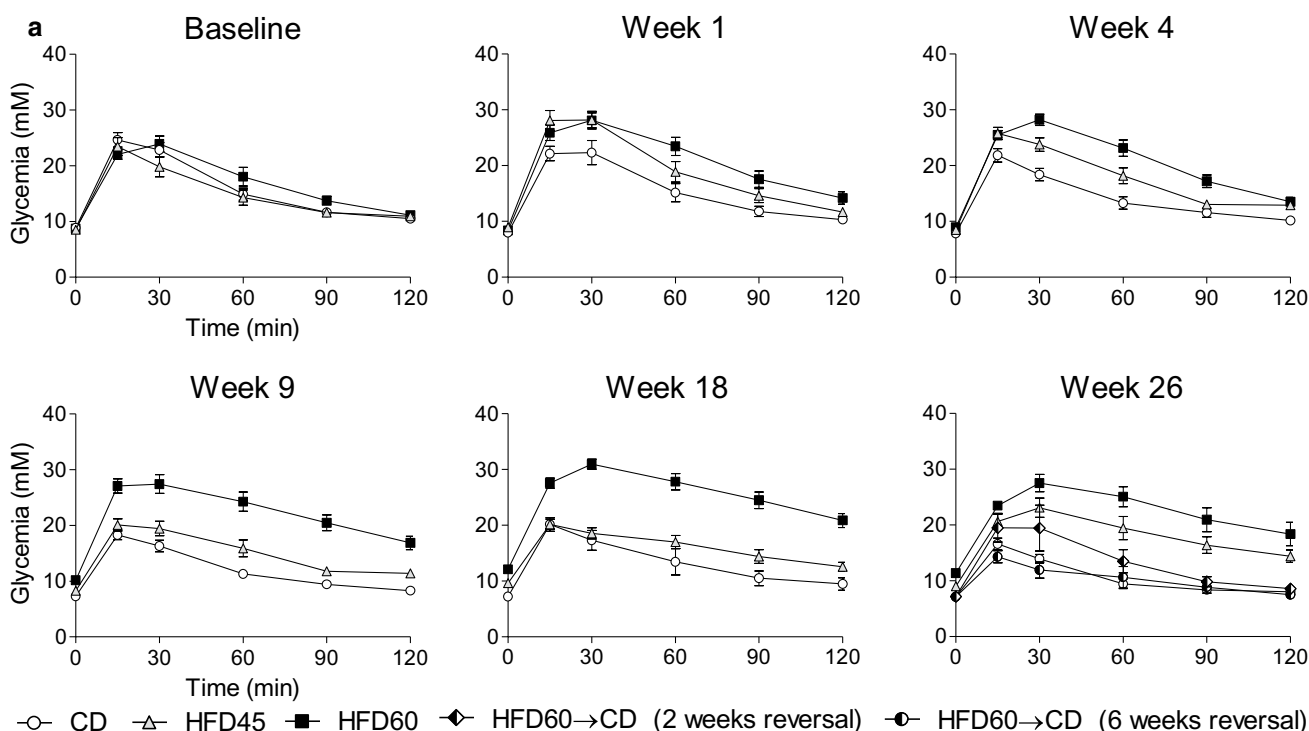
triglyceride levels were similar among all groups (Table 2). Fasting plasma C-peptide levels were higher in the HFD45 and HFD60 groups than in the CD group (Table 2), suggesting increased insulin secretion in HFD-fed mice, in agreement with high fasting plasma insulin levels (Fig. 3d). Increased ALT and AST levels in the blood suggest the presence of liver damage in the HFD45 and HFD60 groups (Table 2). Metabolic variables in the HFD60→CD group were comparable to those in the CD group. However, the values of biomarkers for liver damage (ALT and AST) were in the range observed in the blood of mice in the HFD45 and HFD60 groups (Table 2).

With our longitudinal $^1$H-MRS measurements in vivo, we could monitor changes in hepatic lipids that accompanied the metabolic dysregulation and recuperation induced by the dietary manipulations. Typically, these MR sessions lasted 45–75 min, including animal setup, imaging acquisitions, and liver spectroscopy for HLC and FA composition. At weeks 18 and 26, images acquired from the abdominal region of mice in the HFD60 and HFD45 groups were distinguishable from those of CD mice as the former clearly showed visceral adipose tissue neighboring the liver, which was absent in the latter (e.g., Fig. 4a, b). HLC at the baseline was $(1.4 \pm 0.2)\%$ in the CD group, $(1.2 \pm 0.1)\%$ in the HFD45 group, and $(1.5 \pm 0.2)\%$ in the HFD60 group, as expected for nonmetabolically compromised mice. Accumulation of lipids in the liver can be appreciated in the $^1$H-MR spectra acquired longitudinally in vivo (Fig. 4c), and was noticeable within 4 weeks in both the HFD45 group ($P < 0.01$) and the HFD60 group ($P < 0.05$) when compared with the CD group (Fig. 4d). By week 26, HLC reached $(8.3 \pm 2.7)\%$ in the HFD45 group ($P < 0.05$ vs CD group) and $(17.6 \pm 2.3)\%$ in the HFD60 group ($P < 0.001$ vs CD group). When analyzing grouped data from all the time points, we found significant correlations between HLC and body weight in the CD, HFD45, and HFD60 groups (Fig. 4e–g). In the HFD60 group, strong linearity was observed until week 9 (shown in Fig. 4g), but from week 9 to week 18 a greater increase of HLC with body weight was observed when compared with the previous period. Then, from week 18 to 26, HLC in the HFD60 group increased despite no striking changes in body weight (see also Fig. 2b). In the HFD60→CD group, HLC progressively attained control levels within 7 weeks (Fig. 4g). At the end of the study, HLC was $(2.7 \pm 0.4)\%$ in the HFD60→CD group, similar to that in the CD group [$(2.0 \pm 0.3)\%$, Fig. 4d].

Besides the quantification of HLC, we further characterized the FA composition of hepatic lipids by $^1$H-MRS measurements in vivo acquired with suppression of the water peak (normally visible at 4.7 ppm). In this way, several lipid resonances were revealed (Fig. 5a), from which FA composition indices were derived (Fig. 5b–g). By visual inspection, the hepatic spectral signatures of mice in the HFD45 and HFD60 groups can be distinguished from those of mice in the CD group. Notably, the lipid resonance at 2.8 ppm (Lip 2.8, denoting polyunsaturated bonds) was systematically higher in the HFD45 and HFD60 groups than in the CD group when spectra were scaled for the terminal methyl group at 0.9 ppm (depicted by the arrow in Fig. 5a). The terminal methyl group was used as an internal reference for normalization to one FA chain, as described in the expressions in Table 1. Thus, the calculated MR indices reflect the composition of FA chains in mobile cytosolic lipids, reporting a hypothetical FA with the average chain length and unsaturation characteristics [26]. The average number of double bounds (Fig. 5b) was higher in the HFD60 group than in the CD group at almost all of the time point assessments, and was also higher in the HFD45 group than in the CD group at weeks 9 and 26. This finding was ascribed to an increase of polyunsaturation as denoted by the higher PUFA index (Fig. 5c), while the MUFA index (Fig. 5d) was complementarily reduced and no changes were noted in the SFA index (Fig. 5e) for both HFD regimens. In addition, the mean chain length was greater in the HFD60 group than in the CD group at weeks 4 and 26, and was greater in the HFD45 group than in the CD group at week 26 (Fig. 5f). No differences were observed between groups with regard to the saturation index (Fig. 5g). Dietary switch from HFD60 to CD caused an increase of the MUFA index to control values at week 21 ($P < 0.05$ vs HFD60 at week 18, Fig. 5d). These changes were accompanied by a tendency for a reduction in the SFA index at week 21 ($P < 0.07$ vs HFD60 at week 18) but no changes in the PUFA index. By week 26 all MR indices in the HFD60→CD group were similar to those in the CD group (Fig. 5b–g), indicating similar FA composition of hepatic cytosolic lipids.

Fasting-induced changes in hepatic lipids were investigated in the CD, HFD45, and HFD60 groups after 18 weeks, when a clear metabolic phenotype was observed as described earlier. The response of hepatic lipids to fasting in the HFD60→CD group was assessed after the dietary reversal period, at around week 26. We found higher plasma NEFA concentrations in fasted mice than in fed mice in the CD group ($P < 0.0001$) and the HFD60 group ($P < 0.001$) but not in the HFD45 group or the HFD60→CD group (Fig. 6a). Consistent with a fasting-induced release of NEFA from adipose stores in the CD group, HLC increased more than 1.5-fold with fasting: from $(2.0 \pm 0.2)\%$ to $(5.2 \pm 0.4)\%$ ($P < 0.0001$, Fig. 6b). The same trend was observed for the HFD45 group, with HLC increasing from $(4.2 \pm 0.7)\%$ to $(9.3 \pm 1.2)\%$ ($P < 0.001$, Fig. 6b), while in the HFD60 group, HLC was comparable between the fasted and fed states [$(13.2 \pm 2.5)\%$ and $(11.9 \pm 2.1)\%$, respectively, Fig. 6b]. Fasting-induced hepatic lipid accumulation was restored in the HFD60→CD group, although the

**a** Baseline, Week 1, Week 4, Week 9, Week 18, Week 26 — Glycemia (mM) vs Time (min)

-○- CD  -△- HFD45  -■- HFD60  -◆- HFD60→CD (2 weeks reversal)  -◑- HFD60→CD (6 weeks reversal)

**b** Glycemia 2h-post OGTT (mM) vs Weeks on diet

**c** AUC (arb. units) vs Weeks on diet

**d** Glycemia (mM) vs Weeks on diet

**e** Insulinemia (ug/L) vs Weeks on diet

relative increase was smaller than that in the CD group [from $(2.7 \pm 0.4)\%$ to $(4.5 \pm 0.4)\%$, $P < 0.05$, Fig. 6b].

Fasting-induced changes in HLC were accompanied by alterations of the spectral signature of hepatic lipids assessed by $^1$H-MRS in vivo. There was a noticeable increase of the resonance at 2.8 ppm relative to that of the terminal

methyl group at 0.9 ppm (Fig. 6c), and MR indices related to the unsaturation features of the FA chains were significantly altered between fed and fasted states in the CD group (Fig. 6d). In agreement with the spectral signatures, higher PUFA and lower MUFA indices were observed in fasted mice than in fed mice in the CD group. In the HFD45 group,

◀**Fig. 3** Glucose homeostasis during 26 weeks of exposure to experimental diets. **a** Oral glucose tolerance tests (OGTTs; 1.5 g/kg after a 6-h fast) performed before (baseline, bs) and after 1, 4, 9, 18, and 26 weeks of exposure to the test diets. In the group fed a high-fat diet with 60% of kilocalories from fat for at least 19 weeks followed by the control diet with 10% of kilocalories from fat for 7 weeks (HFD60→CD), an additional test was performed within 2 weeks of dietary reversal, and is represented in the 26-week plot. **b** Blood glucose level 2 h after the OGTT. **c** Area under the curve (AUC) for blood glucose level versus time during the full 2-h OGTT. **d** Fasting blood glucose and **e** fasting plasma insulin levels before the OGTT. The data are the mean with the standard error of the mean and were analyzed with a two-way ANOVA followed by Student's $t$ tests corrected for multiple comparisons when differences from the group fed the control diet with 10% of kilocalories from fat (CD) were assessed across the different time points. One asterisk $P < 0.05$, two asterisks $P < 0.01$, three asterisks $P < 0.001$, four asterisks $P < 0.001$ for high-fat diet with 60% of kilocalories from fat (HFD60) versus CD; one section mark $P < 0.05$, two section marks $P < 0.01$, three section marks $P < 0.001$, four section marks $P < 0.0001$ for high-fat diet with 45% of kilocalories from fat (HFD45) versus CD

there was also an increase of the PUFA index with fasting, together with an increase in the average number of double bounds, but without changes in the MUFA index. No changes of FA composition indices were observed in the HFD60 group with fasting, not even after 7 weeks of reversal to CD (HFD60→CD). Indices for chain length, SFA, and saturation were not significantly altered by fasting in any group (not shown).

## Discussion

This study reports for the first time that changes in hepatic FA composition occur before hepatic steatosis in HFD-fed mice. Importantly, these qualitative changes resembled those caused by fasting, suggesting a similar hepatic response to increased influx of FA. Ectopic lipid accumulation in the liver is a metabolically hazardous feature that accompanies obesity. To better understand the cause of this phenomenon in the scope of obesity-induced metabolic dysregulation, we characterized alterations in hepatic lipids and glucose homeostasis secondary to short-term and long-term exposure to an HFD. Initial exposure to HFD formulas resulted in the immediate development of glucose intolerance, while prolonged exposure led to overt dysregulation of glucose homeostasis and hepatic steatosis. Overall, mice in the HFD60 group developed severer metabolic derangements and faster than those in the HFD45 group, as evaluated from OGTT parameters, fasting plasma insulin and blood glucose values, and HLC. These findings suggest that the amount of fat in the diet influences the degree of ensuing metabolic dysregulation.

We found that glucose tolerance was compromised within 1 week of HFD60 feeding, in good agreement with several studies evaluating short-term effects of HFD

feeding [3, 8, 28–30]. It was previously shown that glucose intolerance induced by an approximately 9-week HFD-feeding protocol can be restored within 1 week by switching to a control diet [31]. Our study now demonstrates that even after longer periods of exposure to an HFD, glucose tolerance is promptly reasserted in response to a reduction in dietary fat intake. However, this finding may be related to the striking decrease of caloric intake observed when the diet was switched from HFD60 to CD, in good agreement with observations from another study [4]. Restricted food intake per se is a strong regulator of glucose homeostasis in HFD models [30, 32] and likely plays an important role in the quick recovery of glucose tolerance in HFD60→CD mice.

During the OGTT, blood glucose level returns to basal values by the action of endogenous insulin. Glucose intolerance has been associated with beta-cell proliferation and hampered glucose-induced insulin secretion after 1 week of HFD feeding [3]. Therefore, an adaptation of pancreatic function could explain the differences in handling a glucose load in the acute HFD60 challenge, relative to CD. In addition to the beta-cell response, sensitivity to insulin action also guides the response to a glucose challenge. Direct assessments of hepatic insulin resistance with hyperinsulinemic–euglycemic clamps have provided evidence of impaired endogenous glucose production after a few days of HFD feeding [8, 9]. This defect also contributes to higher glucose level excursions during the OGTT in HFD-fed rodents [33]. The former studies also report increased HLC after short-term HFD feeding. In this study, we found abnormally high fasting insulin levels, a surrogate of insulin resistance [34], at the same time when hepatic lipid accumulation was detected (i.e., from week 4) in both HFD groups. High fasting insulin levels may indicate a compensatory secretion of insulin (compatible with our C-peptide measurements) in the context of insulin resistance. Distinct experimental conditions (animal's age, dietary fat content, animal housing conditions) may account for the discrepancies regarding the onset of perturbed metabolic events between our study and other studies [8, 9, 29]. Insulin resistance was shown to correlate with liver fat in nonalcoholic fatty liver disease patients [35], and in metabolically healthy men, liver fat was found to be closely associated with fasting insulin levels [36]. Similarly, we previously found a good correlation between liver fat in male mice and their metabolic status [37]. Hyperinsulinemia has been suggested to directly contribute to increased FA uptake by the liver [38], an important mechanism by which lipids accumulate in the liver in HFD models [14, 15, 39]. The progressive decrease of HLC also paralleled the normalization of fasting insulin levels in the HFD60→CD group during the last 7 weeks of the study. Therefore, altogether, these studies confirm a robust association between HLC and insulin resistance/sensitivity.

**Table 2** Metabolic variables after 26 weeks of exposure to experimental diets with different fat contents

| | CD | HFD45 | HFD60 | HFD60→CD |
|---|---|---|---|---|
| EWAT (g) | $0.62 \pm 0.06^a$ | $2.37 \pm 0.10^b$ | $2.32 \pm 0.14^b$ | $0.47 \pm 0.04^a$ |
| Leptin (pg/ml) | $164.6 \pm 13.5^a$ | $581.2 \pm 67.3^b$ | $576.2 \pm 69.7^b$ | $184.7 \pm 13.6^a$ |
| NEFA (mEq/l) | $1.34 \pm 0.18^a$ | $2.42 \pm 0.15^b$ | $2.05 \pm 0.14^b$ | $1.10 \pm 0.26^a$ |
| Triglycerides (mg/dl) | $89.7 \pm 12.5^a$ | $105.5 \pm 6.3^a$ | $99.8 \pm 14.8^a$ | $42.6 \pm 7.2^b$ |
| Glucose (mM) | $9.0 \pm 0.4^a$ | $9.1 \pm 0.4^a$ | $10.8 \pm 0.2^b$ | $8.4 \pm 0.5^a$ |
| C-peptide (ng/ml) | $0.39 \pm 0.24^a$ | $3.32 \pm 1.47^b$ | $2.72 \pm 0.83^b$ | $0.74 \pm 0.52^a$ |
| ALT (U/l) | $21.5 \pm 2.5^a$ | $132.6 \pm 26.8^b$ | $110.5 \pm 18.2^{b,c}$ | $53.6 \pm 11.1^{a,c}$ |
| AST (U/l) | $76.4 \pm 7.0^a$ | $202\ 4 \pm 49.5^b$ | $164.6 \pm 28.2^{a,b}$ | $139.1 \pm 27.3^{a,b}$ |

For each row, values not sharing a common superscript letter are significantly different ($P < 0.05$, one-way ANOVA with the Neuman–Keuls post hoc test). Values refer to mice fed ad libitum except for C-peptide level after a 6-h fast.

*ALT* alanine transaminase, *AST* aspartate transaminase, *CD* control diet with 10% of kilocalories from fat, *EWAT* epididymal white adipose tissue, *HFD45* high-fat diet with 45% of kilocalories from fat, *HFD60* high-fat diet with 60% of kilocalories from fat, *HFD60→CD* HFD60 for 19 weeks followed by CD for 7 weeks, *NEFA* nonesterified fatty acids

Despite the absence of net hepatic lipid accumulation during the first few weeks of exposure to an HFD, we detected significant differences in some indices of FA composition by ^{1}H-MRS in vivo: notably, higher PUFA and lower MUFA indices were observed in both HFD groups when compared with the CD group. These differences are unlikely to reflect the FA composition of the diets, which delivered similar proportions of PUFA sand MUFA in HFD formulas and a greater proportion of PUFA in CD. After overnight fasting, HLC increased in the CD group, as expected [17–19]. This hepatic lipid deposition was accompanied by modifications of the unsaturation indices similar to those induced by an HFD (i.e., increase of PUFA and reduction of MUFA indices).

Increased polyunsaturation of liver lipids with fasting has been reported previously [17, 19], and could reflect the preferential release of PUFA from adipose tissue, as observed in starved rats [40]. However, since PUFA are minor contributors to NEFA after an overnight fast [39], accumulation of PUFA in the liver with fasting seems to be better explained by the privileged uptake and retention of PUFA relative to other FA [17]. This selective accumulation of PUFA in the liver, under conditions of lipid abundance, contributes to curtail intrahepatic SFA levels, thereby limiting SFA-induced lipotoxicity [41]. This mechanism is clearly illustrated by the greater accumulation of lipids in the liver in rats fed a PUFA-rich diet versus rats fed an SFA-rich diet, and the presence of liver damage in the latter but not the former conditions [6]. Reduced MUFA index is consistent with an HFD-induced decrease of stearoyl-CoA desaturase 1 (SCD-1) activity, converting SFA 16:0 and 18:0 to MUFA 16:1 and 18:1 [39, 42, 43]. Moreover, the accumulation of PUFA in the liver both with fasting and HFD challenges will, in principle, have an inhibitory effect on SCD-1 activity [44], thereby also contributing to a reduction of the levels

of hepatic MUFA. The MUFA index immediately increased (along with a tendency for decreased SFA index) when dietary fat content was reduced from 60% of kilocalories to 10% of kilocalories in the HFD60→CD group, in line with a modulation of SCD-1 activity by dietary fat load [43, 44]. Altogether, these data show that the FA composition of liver lipids changes dynamically in adaptation to lipid availability. Situations enhancing hepatic FA uptake (e.g., fasting or an HFD) lead to an immediate increase of PUFA levels in the liver, while a reduction of dietary fat load causes a reduction of the levels of those lipids. Importantly, alterations in hepatic FA composition induced by an HFD were detected before ectopic lipid accumulation in the liver and altered fasting blood insulin and/or glucose levels, which may be of relevance in the anticipation of diet-induced hepatic steatosis and associated metabolic dysregulation.

Early alterations of the hepatic lipid signature by HFD feeding were sustained throughout the study: the PUFA index in HFD-fed mice remained above control levels and the MUFA index remained below them, without striking changes in the SFA index. However, HLC increased significantly with prolonged exposure to an HFD, implying that the absolute levels of both PUFA and SFA increase. In good agreement with our observations, long-term HFD feeding has been shown to increase the amount of PUFA and SFA but not MUFA in hepatic triglycerides [45]. At the end of the study, we also found that the mean chain length was higher in hepatic FA in the HFD45 and HFD60 groups relative to the CD group, in line with increased hepatic FA elongation in long-term exposure to an HFD [45, 46].

Similarly to fasting-induced hepatic lipid accumulation [17, 19, 47], it is the surplus of adipose-tissue-derived-NEFA in the liver that drives hepatic steatosis in HFD-fed rodents [14, 15, 39], as well as in patients with nonalcoholic fatty liver disease [23]. Accordingly, we confirmed
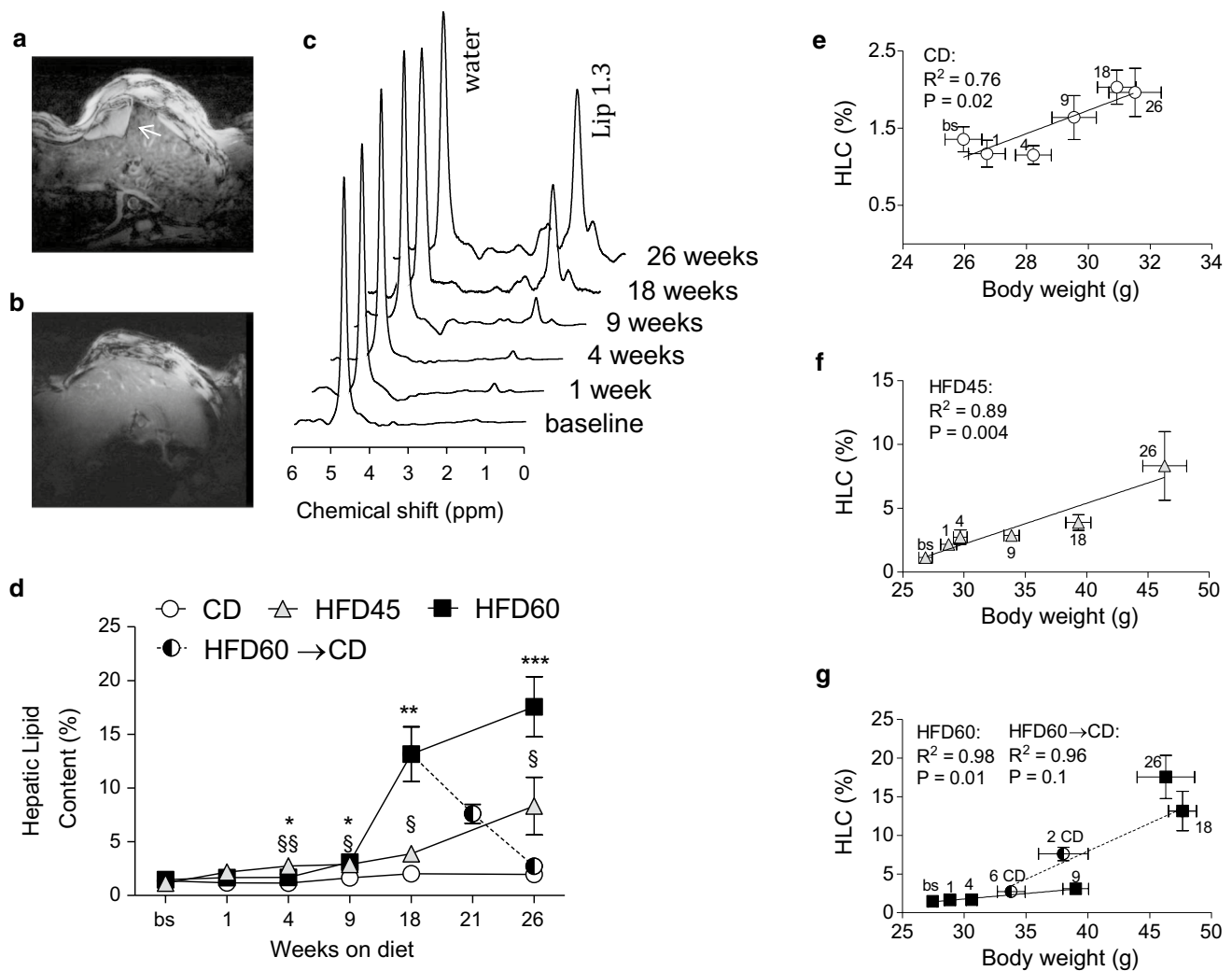
**Fig. 4** Diet-induced changes in hepatic lipid content (HLC) monitored longitudinally by proton magnetic resonance spectroscopy in vivo. Representative sagittal images of the abdominal region are shown for mice after 26 weeks in the group fed a high-fat diet with 60% of kilocalories from fat (HFD60; **a**) and the group fed a control diet with 10% of kilocalories from fat (CD; **b**); visceral fat visible neighboring the liver of an HFD60 mouse is indicated by the arrow. **c** Representative proton magnetic resonance spectra acquired in vivo, longitudinally, from the liver of a mouse in the HFD60 group showing the increase of the fatty acyl proton resonances (0–3 ppm) relative to the water signal at 4.7 ppm. The resonance areas of the methylene fatty acyl protons (Lip 1.3) and water, assigned in the spectra, were used to quantify the HLC. **d** Hepatic lipid accumulation [HFD60 and high-fat diet with 45% of kilocalories from fat (HFD45)] and regression on reversal from HFD60 to CD (HFD60→CD). HLC exhibited a linear relation with body weight in the CD group (**e**), HFD45 group (**f**), and HFD60 group (**g**), as depicted by the full lines. Linearity between HLC and body weight during reversal from HFD60 to CD (HFD60→CD) is depicted by the dotted line in **g**. Goodness of linear fits is denoted by the $R^2$ values in the graphs; $P$ values assessing the difference from null slope are also shown. Numbers next to the symbols in **e–g** indicate the number of weeks for which the mice had been fed the experimental diets. The data are the mean and standard error of the mean, and were analyzed with a two-way ANOVA followed by a Student $t$ test corrected for multiple comparisons. bs baseline. One asterisk $P < 0.05$, two asterisks $P < 0.01$, three asterisks $P < 0.001$ for HFD60 versus CD; one section mark $P < 0.05$, two section marks $P < 0.01$ for HFD45 versus CD

increased EWAT mass and plasma leptin and NEFA levels after 26 weeks in the HFD45 and HFD60 groups, together with hepatic steatosis. Conversely, in response to a relief of the dietary lipid load, the normalization of plasma NEFA and leptin levels in the HFD60→CD group was in good agreement with the reduction of EWAT mass. Reflecting the remodeling of lipid trafficking from adipose tissue to the liver, HLC was also normalized in the dietary switch group

and triglyceride levels were reduced. In contrast to the lack of short-term changes in HLC on exposure to HFD formulas, a few weeks of dietary reversal from HFD60 to CD was sufficient to induce an effective decrease of HLC. This rapid response was also observed in another study that performed a dietary switch from an obesogenic to a control diet [48].

Although not the main focus of this study, visceral fat depots were clearly visible in the MR images acquired at
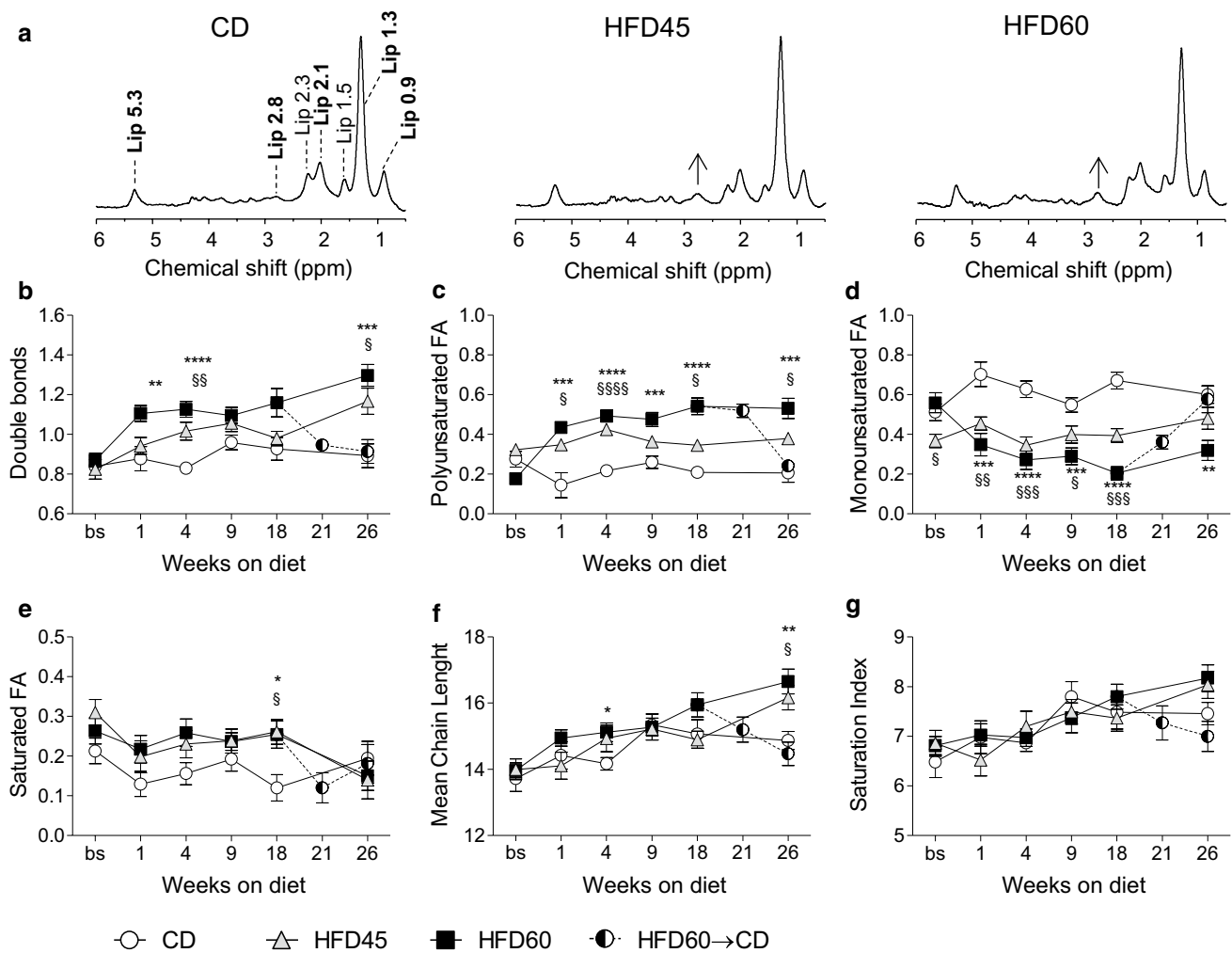
**Fig. 5** Hepatic fatty acid composition monitored by proton magnetic resonance (MR) spectroscopy in vivo. **a** Representative proton MR spectra acquired with water suppression at week 4 from the livers of mice fed a control diet with 10% of kilocalories from fat (CD), a high-fat diet with 45% of kilocalories from fat (HFD45), and a high-fat diet with 60% of kilocalories from fat (HFD60). Resonances from fatty acyl protons are identified in the CD spectrum and are labeled accordingly with their chemical shifts. Bold lettering indicates resonances used to calculate MR indices of fatty acid (FA) composition (Table 1). Spectra are scaled to have the same intensity of Lip 0.9 so

that the relatively higher intensity of Lip 2.8 (depicted by the arrow) in the HFD45 and HFD60 groups in comparison with the CD group can be appreciated. **b–g** Longitudinal evolution of the FA composition indices in the different groups. Data are the mean and standard error of the mean, and were analyzed with a two-way ANOVA followed by a Student $t$ test corrected for multiple comparisons. One asterisk $P < 0.05$, two asterisks $P < 0.01$, three asterisks $P < 0.001$ for HFD60 versus CD; one section mark $P < 0.05$, two section marks $P < 0.01$, three section marks $P < 0.001$ for HFD45 versus CD. HFD60→CD HFD60 for 9 weeks followed by CD for 7 weeks

weeks 18 and 26 in both HFD groups, but not in the CD group. This finding is in line with the notion that visceral fat mediates hepatic lipid accumulation in diet-induced obese mice, with implications for metabolic health [49]. A systematic study on fat depot distribution in mice with appropriate imaging techniques recently showed a strong correlation between visceral fat volume and EWAT mass [50]. In our study, EWAT mass was comparable between the HFD45 and HFD60 groups, but HLC in the HFD60 group was about twice that in the HFD45 group. Presumably, a limited capacity for lipid storage in EWAT

contributes to hepatic steatosis under HFD-feeding protocols.

Most metabolic biomarkers were normalized with the dietary intervention (e.g., glucose tolerance variables, fasting plasma insulin, C-peptide, and blood glucose, HLC, leptin, EWAT). However, transaminase levels were still similar to those in HFD-fed mice, indicating the presence of liver damage. In addition, changes of hepatic lipids with fasting were not fully recovered in comparison with mice not exposed to an HFD. Namely, fasting induced an accumulation of SFA and not necessarily PUFA, suggesting
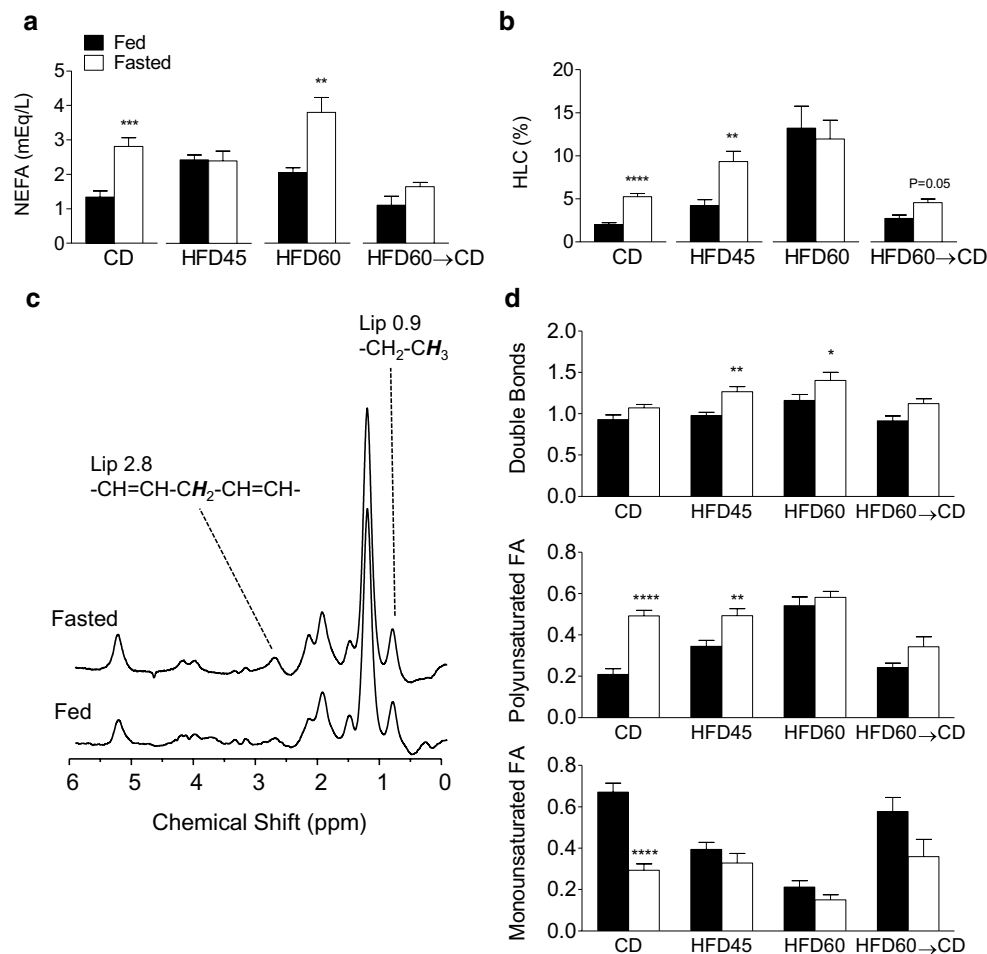
**Fig. 6** Effect of fasting on circulating and hepatic fatty acids. **a** Non-esterified fatty acids (NEFA). **b** Hepatic lipid content (HLC). **c** Representative proton magnetic resonance (MR) spectra acquired in vivo from the liver of one mouse in the group fed the control diet with 10% of kilocalories from fat (CD) in two distinct MR sessions, in the fasted (top) and fed (bottom) states. The major spectroscopic alteration with fasting was the increase of Lip 2.8 relative to Lip 0.9. **d** MR indices of fatty acid unsaturation that showed modulation with fasting. The data are the mean and standard error of the mean. Measurements were performed in mice fed ad libitum (Fed) or mice that had fasted overnight (Fasted) at around week 18 for the CD group, the group fed a high-fat diet with 45% of kilocalories from fat (HFD45), and the group fed a high-fat diet with 60% of kilocalories from fat (HFD60), and at around week 26 after dietary reversal for the group fed HFD60 for 19 weeks followed by CD for 7 weeks (HFD60→CD). Statistical difference between values measured in the fasted state versus the fed state was assessed with a Student $t$ test corrected for multiple comparisons. One asterisk $P < 0.05$, two asterisks $P < 0.01$, three asterisks $P < 0.001$, four asterisks $P < 0.0001$

that mechanisms of FA uptake remain impaired. It is not clear whether a longer dietary reversal period would have allowed a complete normalization of hepatic lipid handling. Several studies report that the resaturation of insulin sensitivity afforded by lifestyle interventions in prediabetes may be transient [35]. In nondiabetic obese patients following a low-caloric diet, the composition of circulating lipids was a predictor for improvements of long-term glycemic control [51]. Thus, whole-body lipid trafficking, as reflected in circulating and hepatic lipid profiles, is an important element accounting for long-term metabolic health.

## Conclusion

In summary, the average polyunsaturation of hepatic FA increases promptly with HFD feeding, independently of the diet's PUFA content, together with a decrease of glucose tolerance, and before net hepatic lipid accumulation is detected. HFD-induced changes in the hepatic FA composition resembled those induced by fasting in mice that received a control diet. Therefore, we conclude from our observations that the hepatic FA composition is an early indicator of whole-body lipid availability, responding to lipid trafficking from adipose tissue to the liver under HFD-feeding protocols. In

addition, because fasting-induced changes in HLC and FA composition were not completely normalized after a dietary intervention, we conclude that whole-body lipid trafficking remains perturbed long after the recovery of other metabolic markers.

**Author contributions** AFS designed the study, performed liver magnetic resonance spectroscopy experiments, collected, analyzed, and interpreted data, and drafted the manuscript. JMND designed the study, edited the manuscript, and contributed to the discussion. RG edited the manuscript and contributed to the discussion.

**Compliance with ethical standards**

**Conflict of interest** The authors declare that they have no competing interests.

**Ethical standards** All procedures performed in studies involving animals were in accordance with the ethical standards of the institution or practice at which the studies were conducted.

# References

1. Swinburn BA, Sacks G, Hall KD, McPherson K, Finegood DT, Moodie ML, Gortmaker SL (2011) The global obesity pandemic: shaped by global drivers and local environments. Lancet 378(9793):804–814
2. Rydén L, Grant PJ, Anker SD, Berne C, Cosentino F, Danchin N, Deaton C, Escaned J, Hammes H-P, Huikuri H, Marre M, Marx N, Mellbin L, Ostergren J, Patrono C, Seferovic P, Uva MS, Taskinen M-R, Tendera M, Tuomilehto J, Valensi P, Zamorano JL, Achenbach S, Baumgartner H, Bax JJ, Bueno H, Dean V, Erol Ç, Fagard R, Ferrari R, Hasdai D, Hoes AW, Kirchhof P, Knuuti J, Kolh P, Lancellotti P, Linhart A, Nihoyannopoulos P, Piepoli MF, Ponikowski P, Sirnes PA, Tamargo JL, Torbicki A, Wijns W, Windecker S, De Backer G, Ezquerra EA, Avogaro A, Badimon L, Baranova E, Betteridge J, Ceriello A, Funck-Brentano C, Gulba DC, Hoes AW, Kjekshus JK, Lev E, Mueller C, Neyses L, Nilsson PM, Perk J, Reiner Ž, Sattar N, Schächinger V, Scheen A, Schirmer H, Strömberg A, Sudzhaeva S, Viigimaa M, Vlachopoulos C, Xuereb RG (2013) ESC guidelines on diabetes, pre-diabetes, and cardiovascular diseases developed in collaboration with the EASD. Eur Heart J 34(39):3035–3087
3. Mosser RE, Maulis MF, Moullé VS, Dunn JC, Carboneau BA, Arasi K, Pappan K, Poitout V, Gannon M (2015) High-fat diet-induced β-cell proliferation occurs prior to insulin resistance in C57Bl/6J male mice. Am J Physiol Endocrinol Metab 308(7):E573–E582
4. Gao X, Yan D, Zhao Y, Tao H, Zhou Y (2015) Moderate calorie restriction to achieve normal weight reverses β-cell dysfunction
5. van der Heijden RA, Sheedfar F, Morrison MC, Hommelberg PPH, Kor D, Kloosterhuis NJ, Gruben N, Youssef SA, de Bruin A, Hofker MH, Kleemann R, Koonen DPY, Heeringa P (2015) High-fat diet induced obesity primes inflammation in adipose tissue prior to liver in C57BL/6j mice. Aging 7(4):256–267
6. Gentile CL, Weir TL, Cox-York KA, Wei Y, Wang D, Reese L, Moran G, Estrada A, Mulligan C, Pagliassotti MJ, Foster MT (2015) The role of visceral and subcutaneous adipose tissue fatty acid composition in liver pathophysiology associated with NAFLD. Adipocyte 4(2):101–112
7. Perry RJ, Samuel VT, Petersen KF, Shulman GI (2014) The role of hepatic lipids in hepatic insulin resistance and type 2 diabetes. Nature 510(7503):84–91
8. Wiedemann MSF, Wueest S, Item F, Schoenle EJ, Konrad D (2013) Adipose tissue inflammation contributes to short-term high-fat diet-induced hepatic insulin resistance. Am J Physiol Endocrinol Metab 305(3):E388–E395
9. Samuel VT, Liu Z-X, Qu X, Elder BD, Bilz S, Befroy D, Romanelli AJ, Shulman GI (2004) Mechanism of hepatic insulin resistance in non-alcoholic fatty liver disease. J Biol Chem 279(31):32345–32353
10. Boon Mariëtte R, Bakker Leontine EH, Haks Mariëlle C, Quinten E, Schaart G, Van Beek L, Wang Y, Van Schinkel L, Van Harmelen V, Meinders AE, Ottenhoff Tom HM, Van Dijk KW, Guigas B, Jazet Ingrid M, Rensen Patrick CN (2014) Short-term high-fat diet increases macrophage markers in skeletal muscle accompanied by impaired insulin signalling in healthy male subjects. Clin Sci 128(2):143–151
11. Bakker LEH, van Schinkel LD, Guigas B, Streefland TCM, Jonker JT, van Klinken JB, van der Zon GCM, Lamb HJ, Smit JWA, Pijl H, Meinders AE, Jazet IM (2013) A 5-day high-fat, high-calorie diet impairs insulin sensitivity in healthy, young South Asian men but not in Caucasian men. Diabetes 63(1):248–258
12. Monetti M, Levin MC, Watt MJ, Sajan MP, Marmor S, Hubbard BK, Stevens RD, Bain JR, Newgard CB, Farese RV Sr, Hevener AL, Farese RV Jr (2007) Dissociation of hepatic steatosis and insulin resistance in mice overexpressing DGAT in the liver. Cell Metab 6(1):69–78
13. Minehira K, Young SG, Villanueva CJ, Yetukuri L, Oresic M, Hellerstein MK, Farese RV, Horton JD, Preitner F, Thorens B, Tappy L (2008) Blocking VLDL secretion causes hepatic steatosis but does not affect peripheral lipid stores or insulin sensitivity in mice. J Lipid Res 49(9):2038–2044
14. Wilson CG, Tran JL, Erion DM, Vera NB, Febbraio M, Weiss EJ (2016) Hepatocyte-specific disruption of CD36 attenuates fatty liver and improves insulin sensitivity in HFD-fed mice. Endocrinology 157(2):570–585
15. Koonen DPY, Jacobs RL, Febbraio M, Young ME, Soltys C-LM, Ong H, Vance DE, Dyck JRB (2007) Increased hepatic CD36 expression contributes to dyslipidemia associated with diet-induced obesity. Diabetes 56(12):2863–2871
16. Brøns C, Jensen CB, Storgaard H, Hiscock NJ, White A, Appel JS, Jacobsen S, Nilsson E, Larsen CM, Astrup A, Quistorff B, Vaag A (2009) Impact of short-term high-fat feeding on glucose and insulin metabolism in young healthy men. J Physiol 587(10):2387–2397
17. Marks KA, Marvyn PM, Henao JJA, Bradley RM, Stark KD, Duncan RE (2015) Fasting enriches liver triacylglycerol with n-3 polyunsaturated fatty acids: implications for understanding the adipose–liver axis in serum docosahexaenoic acid regulation. Genes Nutr 10(6):39
18. Heijboer AC, Donga E, Voshol PJ, Dang Z-C, Havekes LM, Romijn JA, Corssmit EPM (2005) Sixteen hours of fasting

differentially affects hepatic and muscle insulin sensitivity in mice. J Lipid Res 46(3):582–588

19. Langhi C, Baldán Á (2015) CIDEC/Fsp27 is regulated by PPARα and plays a critical role in fasting- and diet-induced hepatosteatosis. Hepatology 61(4):1227–1238

20. Buettner R, Parhofer KG, Woenckhaus M, Wrede CE, Kunz-Schughart LA, Schölmerich J, Bollheimer LC (2006) Defining high-fat-diet rat models: metabolic and molecular effects of different fat types. J Mol Endocrinol 36(3):485–501

21. Duivenvoorde LPM, van Schothorst EM, Swarts HM, Kuda O, Steenbergh E, Termeulen S, Kopecky J, Keijer J (2015) A difference in fatty acid composition of isocaloric high-fat diets alters metabolic flexibility in male C57BL/6JOlaHsd mice. PLoS ONE 10(6):e0128515

22. Nunes PM, Wright AJ, Veltien A, van Asten JJA, Tack CJ, Jones JG, Heerschap A (2014) Dietary lipids do not contribute to the higher hepatic triglyceride levels of fructose-compared to glucose-fed mice. FASEB J 28(5):1988–1997

23. Donnelly KL, Smith CI, Schwarzenberg SJ, Jessurun J, Boldt MD, Parks EJ (2005) Sources of fatty acids stored in liver and secreted via lipoproteins in patients with nonalcoholic fatty liver disease. J Clin Investig 115(5):1343–1351

24. Jonkers RAM, Geraedts TR, van Loon LJC, Nicolay K, Prompers JJ (2012) Multitissue assessment of in vivo postprandial intracellular lipid partitioning in rats using localized $^1$H-[$^{13}$C] magnetic resonance spectroscopy. Magn Reson Med 68(4):997–1006

25. Gruetter R, Tkáč I (2000) Field mapping without reference scan using asymmetric echo-planar techniques. Magn Reson Med 43(2):319–323

26. Soares AF, Lei H, Gruetter R (2015) Characterization of hepatic fatty acids in mice with reduced liver fat by ultra-short echo time $^1$H-MRS at 14.1 T in vivo. NMR Biomed 28(8):1009–1020

27. Tkáč I, Starčuk Z, Choi IY, Gruetter R (1999) In vivo $^1$H NMR spectroscopy of rat brain at 1 ms echo time. Magn Reson Med 41(4):649–656

28. Ji Y, Sun S, Xia S, Yang L, Li X, Qi L (2012) Short term high fat diet challenge promotes alternative macrophage polarization in adipose tissue via natural killer T cells and interleukin-4. J Biol Chem 287(29):24378–24386

29. Lee YS, Li P, Huh JY, Hwang IJ, Lu M, Kim JI, Ham M, Talukdar S, Chen A, Lu WJ, Bandyopadhyay GK, Schwendener R, Olefsky J, Kim JB (2011) Inflammation is necessary for long-term but not short-term high-fat diet-induced insulin resistance. Diabetes 60(10):2474–2483

30. Williams LM, Campbell FM, Drew JE, Koch C, Hoggard N, Rees WD, Kamolrat T, Ngo HT, Steffensen I-L, Gray SR, Tups A (2014) The development of diet-induced obesity and glucose intolerance in C57Bl/6 mice on a high-fat diet consists of distinct phases. PLoS ONE 9(8):e106159

31. Kowalski GM, Hamley S, Selathurai A, Kloehn J, De Souza DP, O'Callaghan S, Nijagal B, Tull DL, McConville MJ, Bruce CR (2016) Reversing diet-induced metabolic dysregulation by diet switching leads to altered hepatic de novo lipogenesis and glycerolipid synthesis. Sci Rep 6:27541

32. Duncan MJ, Smith JT, Narbaiza J, Mueez F, Bustle LB, Qureshi S, Fieseler C, Legan SJ (2016) Restricting feeding to the active phase in middle-aged mice attenuates adverse metabolic effects of a high-fat diet. Physiol Behav 167:1–9

33. Delgado TC, Barosa C, Nunes PM, Cerdán S, Geraldes CFGC, Jones JG (2012) Resolving the sources of plasma glucose excursions following a glucose tolerance test in the rat with deuterated water and [U-$^{13}$C]glucose. PLoS ONE 7(3):e34042

34. Stumvoll M, Mitrakou A, Pimenta W, Jenssen T, Yki-Järvinen H, Van Haeften T, Renn W, Gerich J (2000) Use of the oral

35. Häring H-U (2016) Novel phenotypes of prediabetes? Diabetologia 59:1806–1818

36. Seppälä-Lindroos A, Vehkavaara S, Häkkinen A-M, Goto T, Westerbacka J, Sovijärvi A, Halavaara J, Yki-Järvinen H (2002) Fat accumulation in the liver is associated with defects in insulin suppression of glucose production and serum free fatty acids independent of obesity in normal men. J Clin Endocrinol Metab 87(7):3023–3028

37. Soares AF, Paz-Montoya J, Lei H, Moniatte M, Gruetter R (2017) Sexual dimorphism in hepatic lipids is associated with the evolution of metabolic status in mice. NMR Biomed. doi:10.1002/nbm.3761

38. Steneberg P, Sykaras AG, Backlund F, Straseviciene J, Söderström I, Edlund H (2015) Hyperinsulinemia enhances hepatic expression of the fatty acid transporter Cd36 and provokes hepatosteatosis and hepatic insulin resistance. J Biol Chem 290(31):19034–19043

39. Liu T-W, Heden TD, Morris EM, Fritsche KL, Vieira-Potter VJ, Thyfault JP (2015) High-fat diet alters serum fatty acid profiles in obesity prone rats: implications for in vitro studies. Lipids 50(10):997–1008

40. Raclot T (2003) Selective mobilization of fatty acids from adipose tissue triacylglycerols. Prog Lipid Res 42(4):257–288

41. Viljanen APM, Iozzo P, Borra R, Kankaanpää M, Karmi A, Lautamäki R, Järvisalo M, Parkkola R, Rönnemaa T, Guiducci L, Lehtimäki T, Raitakari OT, Mari A, Nuutila P (2009) Effect of weight loss on liver free fatty acid uptake and hepatic insulin resistance. J Clin Endocrinol Metab 94(1):50–55

42. Wang Y, Botolin D, Xu J, Christian B, Mitchell E, Jayaprakasam B, Nair M, Peters JM, Busik J, Olson LK, Jump DB (2006) Regulation of hepatic fatty acid elongase and desaturase expression in diabetes and obesity. J Lipid Res 47(9):2028–2041

43. Weiss K, Mihály J, Liebisch G, Marosvölgyi T, Garcia AL, Schmitz G, Decsi T, Rühl R (2013) Effect of high versus low doses of fat and vitamin A dietary supplementation on fatty acid composition of phospholipids in mice. Genes Nutr 9(1):368

44. Ntambi JM (1992) Dietary regulation of stearoyl-CoA desaturase 1 gene expression in mouse liver. J Biol Chem 267(15):10925–10930

45. Duarte JAG, Carvalho F, Pearson M, Horton JD, Browning JD, Jones JG, Burgess SC (2014) A HFD suppresses de novo lipogenesis and desaturation, but not elongation and triglyceride synthesis in mice. J Lipid Res 55(12):2541–2553

46. Oosterveer MH, van Dijk TH, Tietge UJF, Boer T, Havinga R, Stellaard F, Groen AK, Kuipers F, Reijngoud D-J (2009) High fat feeding induces hepatic fatty acid elongation in mice. PLoS ONE 4(6):e6066

47. Jaeger D, Schoiswohl G, Hofer P, Schreiber R, Schweiger M, Eichmann TO, Pollak NM, Poecher N, Grabner GF, Zierler KA, Eder S, Kolb D, Radner FPW, Preiss-Landl K, Lass A, Zechner R, Kershaw EE, Haemmerle G (2015) Fasting-induced G0/G1 switch gene 2 and FGF21 expression in the liver are under regulation of adipose tissue derived fatty acids. J Hepatol 63(2):437–445

48. Bidar AW, Ploj K, Lelliott C, Nelander K, Winzell MS, Böttcher G, Oscarsson J, Storlien L, Hockings PD (2012) In vivo imaging of lipid storage and regression in diet-induced obesity during nutrition manipulation. Am J Physiol Endocrinol Metab 303(11):E1287–E1295

49. Foster MT, Softic S, Caldwell J, Kohli R, deKloet AD, Seeley RJ (2013) Subcutaneous adipose tissue transplantation in diet-induced obese mice attenuates metabolic dysregulation while removal exacerbates it. Physiol Rep 1(2):e00015

50. Luu YK, Lublinsky S, Ozcivici E, Capilla E, Pessin JE, Rubin CT, Judex S (2009) In vivo quantification of subcutaneous and visceral adiposity by micro-computed tomography in a small animal model. Med Eng Phys 31(1):34–41

51. Valsesia A, Saris WH, Astrup A, Hager J, Masoodi M (2016) Distinct lipid profiles predict improved glycemic control in obese, nondiabetic patients after a low-caloric diet intervention: the diet, obesity and genes randomized trial. Am J Clin Nutr 104(3):566–575